ARCHIVES OF METALLURGY
Volume 48 2003 Issue 4

ZBIGNIEW GRONOSTAJSKI*, KAROL JAŚKIEWICZ*

THE EFFECT OF COMPLEX STRAIN PATH ON THE BEHAVIOUR OF CuSi 3.5 SILICON BRONZE

WPŁYW ZŁOŻONEJ DROGI ODKSZTAŁCANIA NA ZACHOWANIE SIĘ BRĄZU KRZEMOWEGO CuSi 3,5

The effect of tempearture, strain rate and strain on the structure and plastic properties of metals and alloys has been widely known, and improvement of above mentioned features by changes of deformation conditions only has been rather exhausted, but the effect of strain path changes is less known especially in the case of massive processes. Therefore the effect of different complex strain paths on behavior of CuSi3.5 silicon bronze has been investigated. The strain paths contain various sequences of cyclic torsion and monotonic tension were applied. The amplitude was changed in the range of 0.01-0.6, temperature 20-800 °C and strain rate 0.01-1 s^{-1}. The platic properties and structure obtained in complex strain paths were compared with those gained in monotonic torsion and tensile tests. The silicon bronze containing about 3.5 % Si has a very low stacking fault energy, therefore in the mechanism of complex deformation the twinnings and crystalographic slip play the imporatant role. The strain paths similar to those applied in the experiments are observed in some industrial processes. By proper chosen of the strain path the control of the flow stress and the limit strain can be obtained.

Keywords: complex strain path, silicon bronze, plastic properties

Wpływ temperatury, prędkości odkształcania i wielkości odkształcenia na strukturę i plastyczne właściwości metali i stopów jest szeroko poznany i możliwość poprawy tych właściwości poprzez ww. parametry odkształcania jest praktycznie wyczerpana. Jedynym istotnym czynnikiem, którego wpływ nie jest jeszcze dokładnie przebadany jest zmiana drogi odkształcania, szczególnie w procesach obróbki objętościowej. Celem pracy było zbadanie zachowania się brązu krzemowego CuSi3.5 pod wpływem różnych dróg odkształcania. Drogi odkształcania obejmowały różne sekwencje skręcania małocyklowego i monotonicznego rozciągania. Amplitudę zmieniano w zakresie od 0.01 do 0.6, temperaturę od 20 do 800 °C i prędkość odkształcania od 0.01 do 1 s^{-1}. Wyniki uzyskane po odkształceniu złożonym porównano z wynikami otrzymanymi w monotonicznym skręcaniu i rozciąganiu. Brąz krzemowy zawierający około 3.5 % Si jest stopem o bardzo niskiej energii błędu ułożenia, stąd ważną rolę w mechanizmie odkształcania w złożonych drogach

* POLITECHNIKA WROCŁAWSKA, 50-371 WROCŁAW, UL. ŁUKASIEWICZA 3/5

odkształcania odgrywa bliźniakowanie i krystalograficzny poślizg. Podobne drogi odkształcania, do analizowanych w pracy, występują w niektórych procesach przemysłowych. Zaobserwowano, że poprzez właściwy wybór drogi odkształcenia możliwe jest sterowanie naprężeniem uplastyczniającym, odkształceniem plastycznym oraz strukturą odkształcanego materiału.

1. Introduction

The flow stress-plastic strain relationship is basic properties of materials in numerical simulation of materials behavior in forming processes. The effect of temperature, strain rate and strain on the flow stress and structure has been widely investigated and known. Therefore, when new generation of computers and commercial FEM programmers create the possibilities to solve even very complicated forming processes with high accuracy, the meaning of proper work hardening curves is duly appreciated. In the past such processes could be solved mainly for the perfectly plastic model of materials. As progress in computers was made the new factors effected work hardening curves were introduced into it. The base new factor is the strain path.

The effect of strain path in the case of sheet metals forming processes has been investigated for a longer time. It has been found that the effect is very important, so it is even difficult to use forming limit diagrams (FLDs) in sheet metal forming processes design without taking into account the strain path (Fig. 1). For the linear strain path the forming limit is given by curve (1), for the first complex strain path it is composed from the uniaxial tension in the first step of deformation and equibiaxial stretching in the second one as shown curve (2) and for the second complex strain path the sequence of kind of deformations is reverse (curve 3). From that figure it can be seen that the effect of strain path changes is distinct, and the highest limit strain is obtained for curve (2). In both complex strain paths analysed the change of strain direction is equal to 90°. In the case of aluminium sheet it has been found that for strain path changes to have a significant effect the path change should be at least 90° [1]. Then there is substantial response of the dislocation sub-structure to the

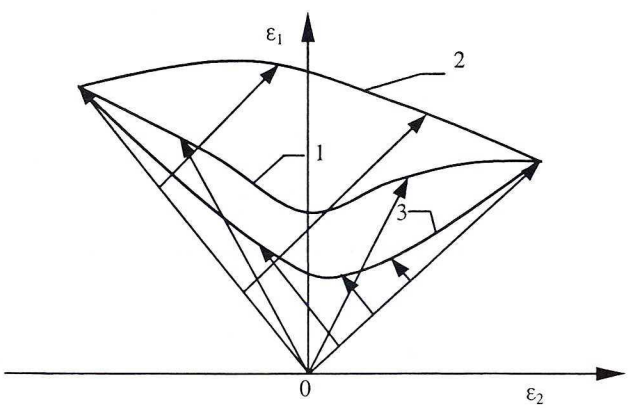

Fig. 1. The FLD for different strain paths

changes in strain path. The cell walls tend to form in orienatations such that they deform less than the overall body. When a deformation involving a large strain path change is imposed on a stucture containing such cell walls, the possibility of geometric accomodation is reduced and the preexisting walls are subject to high stresses. The walls are disrupted, probably by shearing across an essentially dipolar structure. Besides the effect of strain rate on the flow stress is diminished after a large change in strain path. The elimination of the rate sensitivity of strain hardening is due to the cell walls being disrupted by an essentially athermal process following a path change. The normal recovery process occuring in cell walls to accommodate the glide dislocations, which give rise to the rate sensitivity of strain hardening, are no longer as relevant [1].

In the case of massive processes the effect of strain path on the plastic properties and structure of materials is less known because an investigations are more difficult and complex. Only a small number of experiments concerning the effect of strain path changes on behavior of metals and alloys were performed.

The response of a material to changes in strain path depends on a number of factors [2]:

- the microstructure, particularly connected with level of the stacking fault energy,
- the presence of precipitates or second-phase particles,
- the temperature and strain rate history of deformation.

The results of S t o u t and R o l l e t t [3] show that the effect of strain path depends very strongly on dislocation sub-strucrure developed during the deformation of aluminium base alloys. Since the nature of the dislocation sub-structure depends on the stacking fault energy, therefore this factor controls material response to strain path changes.

The presence of precipitates or particles are important both for their effect on the stability of the dislocation sub-structure and on their interaction with the disclocation and that way it reduces the effect of the strain path changes. But with growth of temperature and strain rate the effect of precipitates or second-phase being treated as sub-categories. The temperature and strain rate history of the deformation have effect on the internal state of material even for the same final equivalent plastic strain.

The main categories for discussing strain path effects on the flow stress and structure seem to be:

- the kind of strain path, that is: strain reversal or other strain path changes,
- the value of plastic strain, that means large or small, dividing line should be at plastic strain equal to about 1,
- the value of the effective strain in each strain path changes.

In the last years in massive processes the cyclic torsion (CT) versus monotonic torsion (MT) is often used to show the effect of complex strain paths (CT) on the behaviour of metals and alloys during deformation. In such deformation Bauschinger effect takes place, but in the case of more complex deformation this effect is somewhat misleading since it implies a single mechanism, whereas it should refer to a single observation that arises from a different causes. Therefore it would be beter to refere to it as the B a u s c h i n g e r observation [1]. The most precise definition of this term is that it referes to a transient decrease in work hardening rate upon reversal of the direction of loading. From the wider point of view of the strain path changes effect on the flow stress and structure each change of

the loading direction, not only reversal change should be taken into account. The flow stress is a function of dislocation motion, which is affected by dislocation interactions and microstructural features created by them and the change of principal stress orientation ought to has an influence on the dislocation motion.

The softening as well as hardening during low cyclic deformation can be observed as a function of cumulative plastic strain in succesive cycles or as a number of cycles (Fig. 2 and 3) [4].

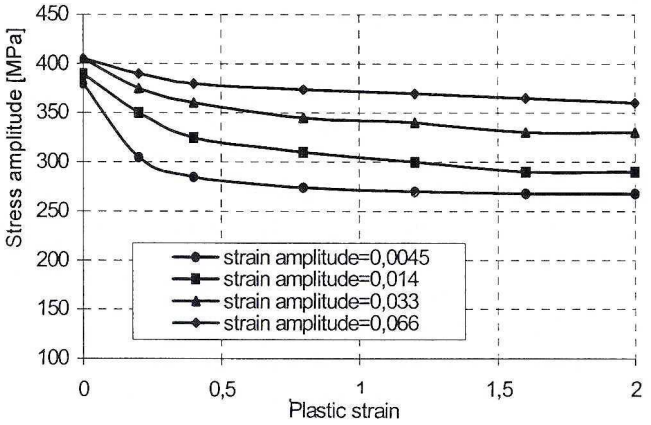

Fig. 2. Low cyclic softening of copper after initial deformation at ambient temperature [4]

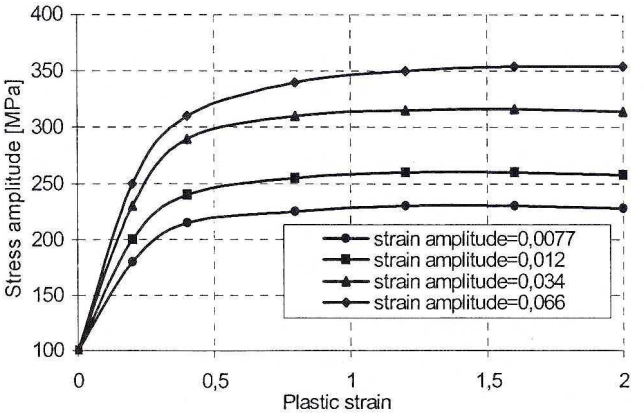

Fig. 3. Low cyclic hardening of anealing copper [4]

If for constant total strain amplitude ε_{at} or plastic strain amplitude ε_{ap}, the flow stress decreases with deformation until saturation stress is reached that is softening of materials (Fig. 4a), but when it grows that is hardening (rys. 4b), and if it is constant that the steady state of flow stress is reached (Fig. 4c) [5].

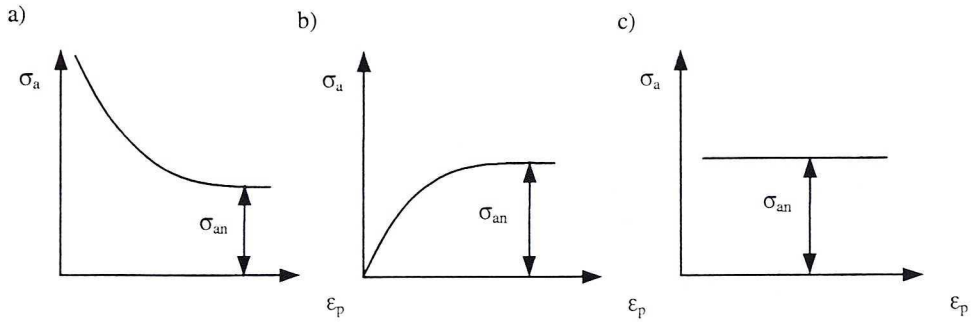

Fig. 4. Behaviour of materials at ε_{ac}=const: a) softening, b) hardening, c) steady state [5]

The relationship of the saturation stress σ_{an} and the plastic strain amplitude ε_{ap} creates the cyclic deformation diagrams. The comparison of low cyclic deformation diagrams with work hardening curve in tensile test is shown in Fig. 5.

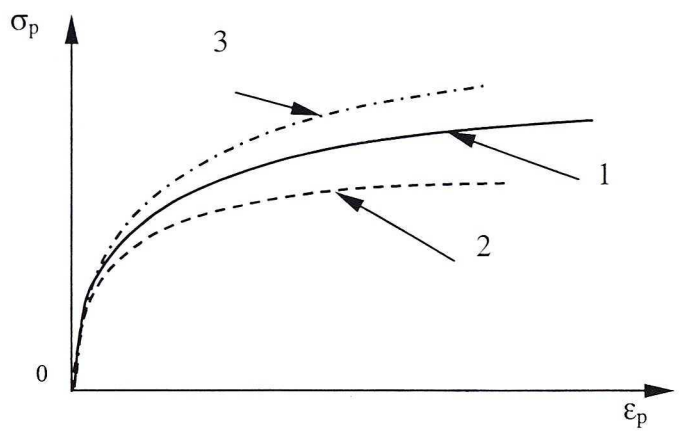

Fig. 5. The comparison of low cyclic deformation curves: 1-curve obtained in tensile test, 2-softening curve, 3-hardening curve

The reciprocal position of flow strsss-plastic strain curves (1), (2) and (3) gives information about the effect of low cyclic deformation on the posibilities of realisation of more efficient metal forming processes.

In the paper [6–9] authors present the stress-strain curves of commercially pure copper and interstitial free steel obtained in hot cyclic torsion test with strain amplitude range of 0.025-0,4 and compare them with curves determined in monotonic test at the same temperature of 500 °C and strain rate of 0.1 s^{-1}. The stress-strain curves for cyclic torsion are significantly different from those of monotonic loading tests. The cyclic torsion stress-strain curves did not show the peak stress characteristic of dynamic recrystallization, suggesting the absence of this phenomenon. The authors show that the cyclic steady state stress with increase of strain amplitude is quite close to that corresponding to the monotonic dynamic recrystallization steady state flow and for highest strain amplitude used in the

experiments (0.4) no increase of the cyclic steady state stress above the steady state flow was observed.

The results shown in above mentioned papers concern small range of deformation below 2.5 only, at larger deformation for CuAl8 aluminium bronze obtained by using complex plastometer even for the same amplitude equal to 0.4, the cyclic steady state stress above the monotonic dynamic recrystallization steady state flow was observed [10, 11]. The another investigations where samples were simultaneously monotonic tension and cyclic straining by torsion with different amplitudes and various sequences shows that relationship between cyclic steady flow stress and steady state flow stress is dependent on the cumulative plastic strain [12].

The results presented in papers [6-9] have serious reservation. During cyclic deformation each hysteretic loop contains elastic and plastic deformations, and the lower deformation amplitude and the more cycles in the whole deformation process the elastic strain in the total deformation increase more rapidly than in the monotonic tests. Therefore the comparison of the flow stress-total strain relationship in cyclis deformation and monotonic torsion or tension can not be done. For proper comparison of above-mentioned curves the elastic deformation must be removed from the total deformation of cyclic as well as monotonic flow stress-strain relationship.

The other works [13–15] contain the experimental characteristic of flow stress of metallic materials in various deformation conditions and theoretical analysis of plastic flow identification during change of the strain paths. Such information can be used in the numerical simulation of metal forming processes especially for no monotonic and no proportional flow of materials. The investigation of change of principal strain orientation on the course of M1E copper, titanium alloy Ti-3,5Al-1,5Mn and OH18N9 steel confirmed the essential influence of strain path changes on the forces needed for deformation, and that way on the work hardening curves [13–15]. The following variants of deformation were used: torsion-tension-torsion in the same direction as before, torsion-tension – torsion in the reverse direction as before, and torsion-torsion-torsion with change of direction in each successive cycle. In each variant of the deformation the same value of total strain was applied, it was equal to 0.3. It means that in each deformation cycle the strain was 0.1. The obtained curves were shown in Figs. 6–8.

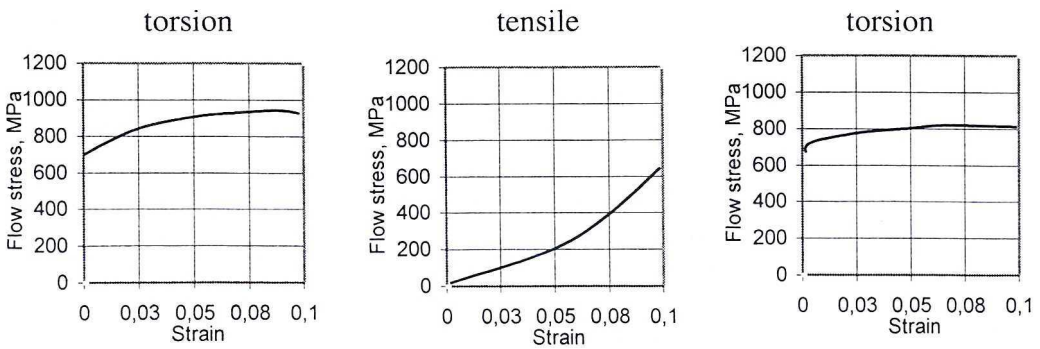

Fig. 6. Relationship between flow stress and strain for titanium alloy for first variant of complex deformation [13]

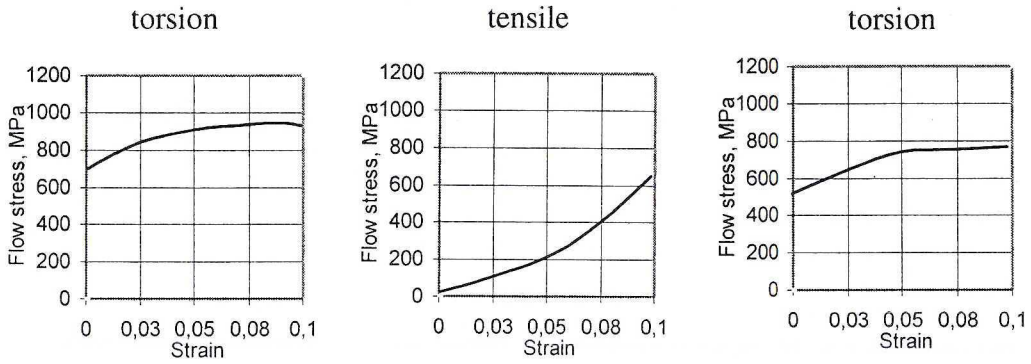

Fig. 7. Relationship between flow stress and strain for titanium alloy for second variant of complex deformation [13]

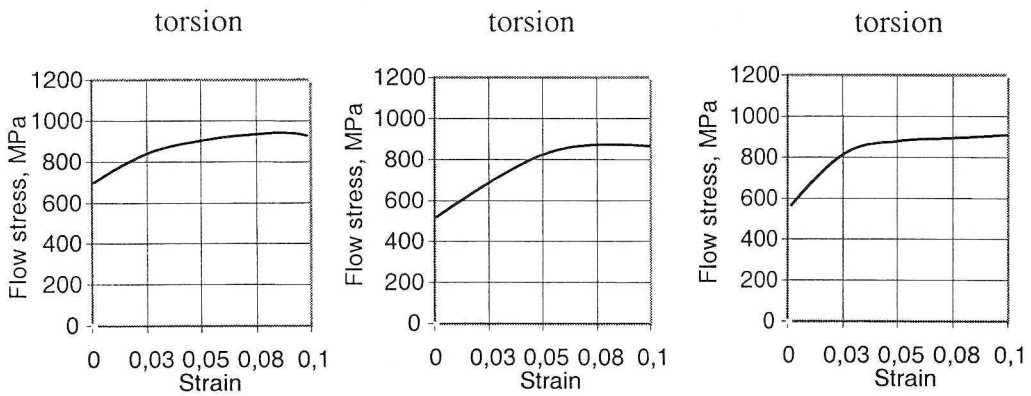

Fig. 8. Relationship between flow stress and strain for titanium alloy for third variant of complex deformation [13]

From that figures it can be seen that after work hardening by torsion, in the tensile test the flow stress-strain relationship is nearly linear. The renewed torsion, in the same direction as before, caused further increase of the flow stress in comparison with that in tensile test, but the maximum value obtained in third cycle of deformation (torsion) is little bit lower than in the first one.

In the second variant of the deformation the change of torsion direction in the third cycle causes significant decrease of the flow stress in comparison with that in first cycle (torsion) (Figure 7).

In the case of successive change of torsion direction (third variant of deformation) the maximum flow stress is stabilized on the same level in the first and third cycle of the deformation, when torsion is realized in the same direction. But in the second cycle when torsion direction is reverse the small decrease of the flow stress can be seen. In above describe papers there is no information if the total strain or plastic strain was used. It is also difficult to imagine that the differences between work hardening curves in the first torsion

and the next tension could be so large as is shown in Figs. 6 and 7. On the base of above presented results the laboratory and industrial energy saving processes by control of strain path changes were proposed [13–15].

The similar investigations [16] for brass containing:, 35.6 %Zn, 0.32 %Sn, 2.8 %Pb, rest Cu were performed for three sequences of strain paths: tension-torsion, torsion-tension and tension-torsion-tension. Monotonic tension and torsion were also completed in order to obtain a baseline comparison for sequence tests. The tests were conducted at room temperature and at an initial strain rate of 0.0631 s^{-1}. It has been found that monotonic torsion leads to less hardening than monotonic tension. The similar results were obtaned in papers [17, 18], where it has been found that in FCC aloys with low SFE the strain hardening rate in the shear deformation is much lower than that in monotonic tension. Such behavior of 70/30 brass with low SFE, was confered by the normalized relationship between equivalent strain harednning rate $(d\sigma_p / d\varepsilon_p)/G$ and the indicator of dislocation density that is built in the metal during the deformation process $(\sigma_p - \sigma_0)/G$ (Fig. 9). From the figure it can be seen the lower strain haredening for monotonic torsion than for monotonic compression. Tension-torsion and torsion-tension strain path changes lead to opposite behaviors. The effect of strain path changes depends on the deformation sequence and on the strain magnitude at the path transition. The effects of path changes can be probably associated with the various slip modes and dislocation structures of different materials.

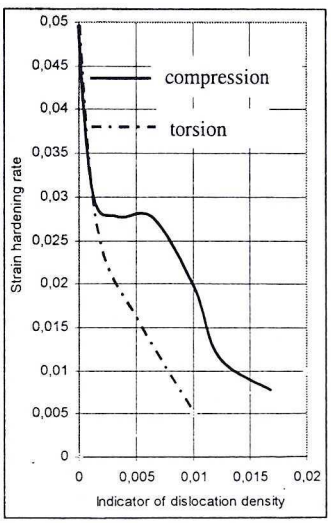

Fig. 9. Normalized strain haredening response of annealed 70/30 brass in monotonic compression and torsion tests

The reversal of deformation of pure aluminium might reduce the dislocation density of cell walls without affecting their orientations, whereas orthogonal changes lead to an overall change in the orientation of the walls. In this manner, reversal of deformation would have the greater effect on that aspect of microstructure, which determines recrystallization

kinetics during annealing of aluminium after deformation, namely by the energy associated with the recovered cell wall structures [19].

In the other work [20] the less hardening and the small strain hardening rates in the pure shear of FCC materials than in the simple tension can be atributed to the different distribution of strain in cross section of torsioned sample and conected with this various distribution of temperature.

In this literature review the investigations of the strain path changes on the behavior of metals and alloys were described. The works indicate that strain path effects are real and cannot be dealt with by simple formulation invoking net or cumulative strain. It is clear that microstructural evolution during the deformation is influenced by the strain path. The described works have been focused on sequential path changes mainly at room temperature, sbut the obtained results are not the same. The effect of high temperatures and strain rates is even less known and should be clarified because there is some similarity between the results of various experiments and industrial practices as: rolling [21], ingot turning [22], rotary forging [23], rotary swaging [24], extrusion [25] and other processes, where the strain path changes are observed.

From above discussion it is clear visible that by change of the strain path in a massive processes the great progress in metal forming processes can be obtain and new technologies more efficient from the point of view of energy and material consumption can be elaborated.

The main aim of the paper is to analyse the complex strain path effect on the behavior of CuSi3.5 silicon bronze during plastic deformation in the wide range of deformation conditions.

2. Experimental procedure

For the plastic properties evaluation the plastometer for complex strain paths (Fig. 10) was used [26]. The specimens made from CuSi3.5 silicon bronze were deformed in the temperature range of 20–800 °C. The temperature was measured by a thermocouple in contact with surface of the gage length of the specimens. The specimens were monotonic tension with the strain rate of 0,01 s^{-1} simultaneously with symmetrical cyclic torsion with the strain rate of 0.1 s^{-1} and different total amplitudes ε_{ac}= 0.05, 0.1, 0.2, 0.3, 0.4, 0.5 and 0.6. For comparison the pure monotonic torsion and tension were performed with strain rate of 0.1 s^{-1}. For microstructural observation the optical, scanning and electron microscopes were used. The specimens shown in fig. 11 were used in experiments.

As it was explained in the former chapter for proper determination of the effect of strain paths on the flow stress-plastic strain relationship and on the limit strain the elastic deformation must be removed from the total deformation. The method of partition of total strain during complex deformation on elastic and plastic parts is shown in the Figure 12. The elastic and plastic strain in succeeding hysteresic loop were calculated using courses of

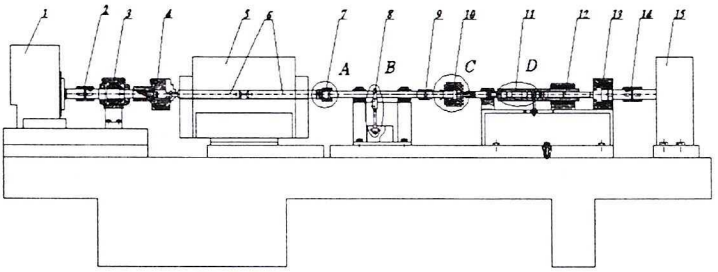

Fig. 10. Scheme of plastometer: 1 – asynchronous machine of 13 kW power, 2 – sleeve clutch, 3 – constans support, 4 – swivel head, 5 – furnace, 6 – sample holder, 7 – self-centric clutch, 8 – torque sensor, 9 – cluch, 10 – rotanion head, 11 – compresion and tensile sensor, 12 – screw mechanism, 13 – constant support, 14 – sleeve clutch, 15 – asynchronous machine of 13 kW power

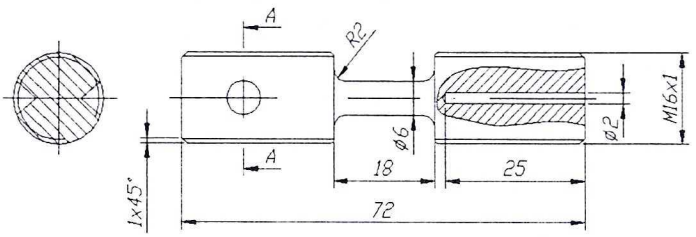

Fig. 11. The scheme of specimens used for complex strain paths

the total strain as a function of time put together with the courses of flow stress in the same time. From that figure it can be seen that the zero values of torsion flow stress correspond finite values of strain. When the torsion flow stress is equal to zero the power transmission system, recording system and specimen are loading only by tensile flow stress σ_{pr}, so at assumption that stiffness of whole plastometer is much higher than deformed specimen alone, the strain of the sample contains plastic deformation caused by torsion ε_{ptl} and total tensile deformation ε_{crl}. For known Y o u n g module E the elastic deformation caused by tension can be easy calculated $\varepsilon_{srl} = \sigma_{pr}/E$. Finally the plastic strain caused by torsion and tension ε_{ptrl} at sucessive half cycles of deformation is given by following formula $\varepsilon_{ptl} + \varepsilon_{crl} - \varepsilon_{srl}$ (Figure 12a).

Values of flow stress and strain shown in Figure 12 are quite optional to illustrate only the way of calculation of plastic strain in low cyclic complex deformation processes. The total plastic strain is cumulative of plastic strain in successive half cyclic of deformation. In the Fig. 12 the effective flow stress determined from equation (5) is shown by dotted line. The BASIC programme for calculation of plastic strain in complex strain paths processes according to above metioned procedure was elaborated.

Till now the universal method of stress and strain calculation in torsion test has not been elaborated yet. There are a few of the different methods given in the papers [27–29]. Taking into account that the main aim of the work is the comparison of flow stress strain curves

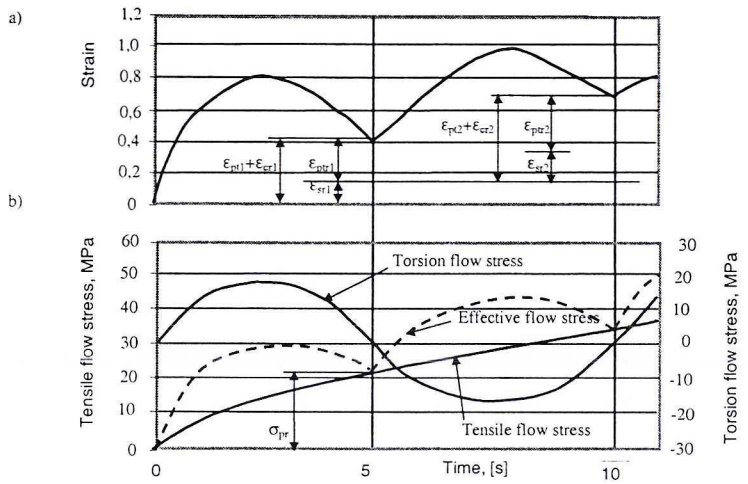

Fig. 12. Complex low cyclic courses: a – strain and b – stress as a function of time for complex deformation process containing cyclic torsion with monotonic tension

obtained in complex strain path with those of monotonic strain, the simple classical method of flow stress and strain determination was used.

In the method the shear stress determined by

$$\tau_p = \frac{M_s(3 + n + m)}{2\pi r_{or}^3} \tag{1}$$

was simplified by omission of work hardening coefficient n and strain rate sensitivity coefficient m

$$\tau_p = \frac{3M_s}{2\pi r_{or}^3}, \tag{2}$$

where: M_s – torque,

r_{or} – real outer specimen radius.

In calculation the real outer specimen radius must be used because the length of specimen is increase by tensile force F.

The differences in the values of the flow stress caused by by omission of work hardening coefficient n and strain rate sensitivity coefficient m are very small and exist mainly in the range of maximum stress (Fig. 13).

The flow stress determined in tensile test is given by

$$\sigma_{pr} = \frac{F}{2\pi r_{or}^2}, \tag{3}$$

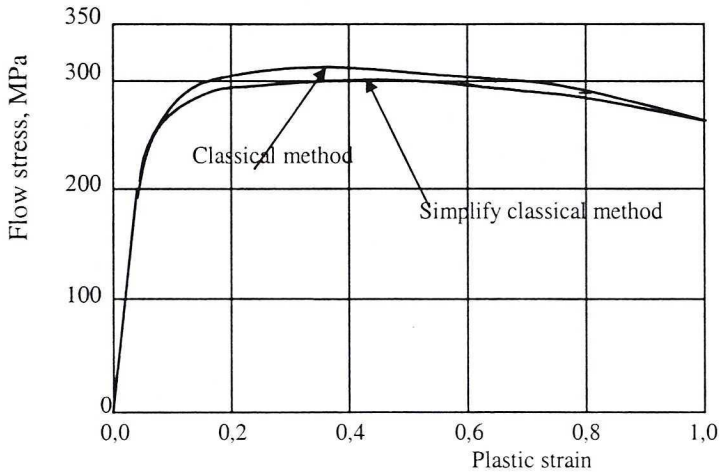

Fig. 13. Relationship between work hardening curves calculated by using classical method (1) and simplifies classical method (2) [15]

The equivalent stress comes from simultaneously operating torsion and tension calculated according to H u b e r - M i s s e s criterion is given by

$$\sigma_{pe} = \sqrt{\sigma_{pr}^2 + 3\tau_p^2}. \tag{4}$$

Substitute (2) and (3) into (4) the equivalent stress in complex deformation is obtained

$$\sigma_{pe} = \sqrt{\left(\frac{F}{2\pi r_{or}^2}\right)^2 + \left(\frac{3\sqrt{3}M_s}{2\pi r_{or}^3}\right)^2}. \tag{5}$$

The equivalent plastic strain determined also according to H u b e r - M i s e s criterion is as follows

$$\varepsilon_{pe} = \frac{1}{\sqrt{3}}\sqrt{3\varepsilon_p^2 + \gamma_p^2}, \tag{6}$$

where: ε_p – strain caused be tensile force F, calculated according to

$$\varepsilon_p = \ln\frac{l_k}{l_p} \tag{7}$$

and γ_p – shear strain caused by torque M_s

$$\gamma_p = \frac{r_{or}\omega_p}{l_k} \tag{8}$$

where: l_p and l_k – initial and final gauge length of specimen respectively,
ω_p – angel of plastic rotation of sample,
The strain rate in torsion is given by

$$\dot{\gamma} = \frac{r_{or}\dot{\omega}_p}{l_k} \tag{9}$$

and in tension by

$$\dot{\varepsilon} = \frac{d\varepsilon}{dt}, \tag{10}$$

where: $\dot{\omega}$ – rotational speed.
The equivalent strain rate for these tests is given by

$$\dot{\varepsilon}_e = \frac{1}{\sqrt{3}}\sqrt{3\dot{\varepsilon}_p^2 + \dot{\gamma}_p^2}. \tag{11}$$

3. Results and discussion

The equivalent flow stress – plastic strain relationships obtained in the complex minor symetrical cyclic torsion with different amplitudes simulteneously deformed by monotonic tension, in monotonic torsion and in monotonic tension at ambient temperature are shown in Fig. 14 and at 600 °C in Fig. 15.

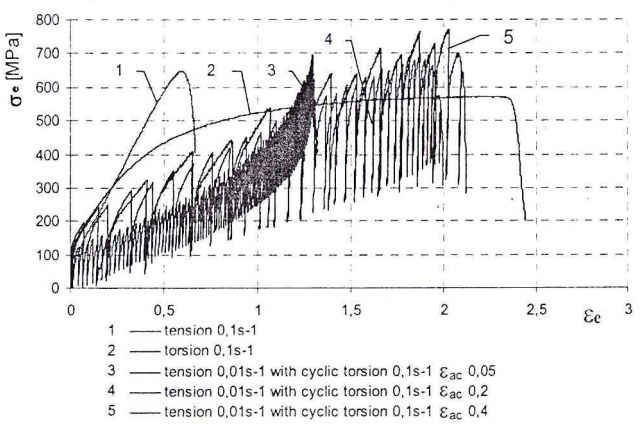

Fig. 14. The effect of application of symmetrical minor cyclic torsion with three different amplitudes during tension of specimens on the relation between equivalent stress and strain in comparison with monotonic tension and torsion at ambient temperature

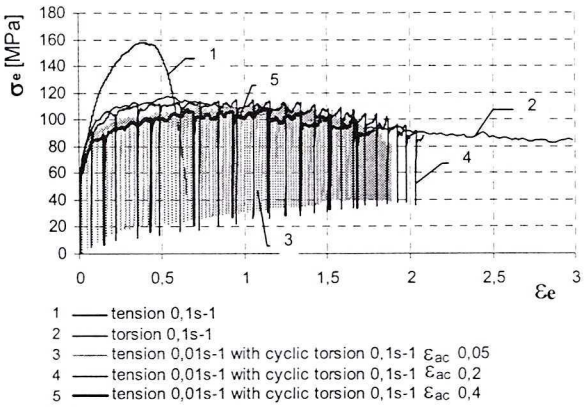

Fig. 15. The effect of application of symmetrical minor cyclic torsion with three different amplitudes during tension of specimens on the relation between equivalent stress and strain in comparison with monotonic tension and torsion at 600 °C temperature

From Fig. 14 it can be seen that at room temperature at small deformation below 0.6 of equivalent plastic strain, the equivalent flow stress in tensile test is much higher than that obtained in complex deformation and below 1.2 of equivalent plastic strain the equivalent flow stress in torsion test is also higher than equivalent flow stress in the same complex deformations. At the higher equivalent plastic strain the all complex deformations cause the increase of highest values of equivalent flow stress above the monotonic torsion flow stress. The greater increase of flow stress for smaller cyclic amplitude (ε_{ac}= 0.05) than for the higher one (ε_{ac}= 0.4) is observed.

Fig. 16. CuSi3.5 silicon bronze structure at room temperature after monotonic tension to ε_p=0.5 with strain rate of 0,1 s^{-1}

The initial structure of CuSi3.5 silicon bronze contains equiaxial grains of average diameter equal to about 250 μm. After monotonic tension at ambient temperature the structure contains a lot of twins and slip lines obtaned mainly by one active slip system oriented parellel to the direction of maximum shear stress. Note that studied silicon bronze has FCC crystallographic structure and both slips and twinnings occur only on (111) planes, and therefore when the twins are parallel to the imposed shear planes, it is resonable to assume that these twin plates are coplanar with the active slip planes. The stucture has not even traces of micro-scale shear bands (Fig. 16). It means that base mechanism of deformation at room temperature is twinning and crystalographic slip. Similar structure was obtained after monotonic torsion. If additional cyclic torsion is introduced to tension the two set of intersecting slip systems are activated on (111) planes where the imposed maximum shear stresses were existed (Fig. 17) and the few micro-scale shear bands appear (Fig. 18).

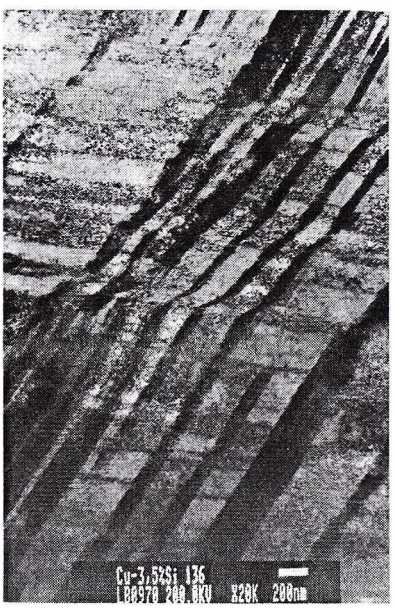

Fig. 17. Two set of reciprocal intersecting twinings in CuSi3.5 silicon bronze at room temperature deformed to ε_p=0.8 with strain rate of 0,1 s^{-1} and strain amplitude of 0.2

The increase of temperature to 600 °C strongly effects the courses of equivalent flow stress-equivalent plastic strain relationships (Figure 15). The equivalent flow stresses for all applied strain paths are nearly the same, beside the equivalent tensile flow stress at small deformation where it obtaines the highest values. The equivalent flow stress-equivalent plastic strain curves have not maximum of the flow stress characteristic for the dynamic recrystallization, which are usually seen in the monotonic curves. The reason of such behavior of silicon bronze is that the applied complex deformation causes the cyclic

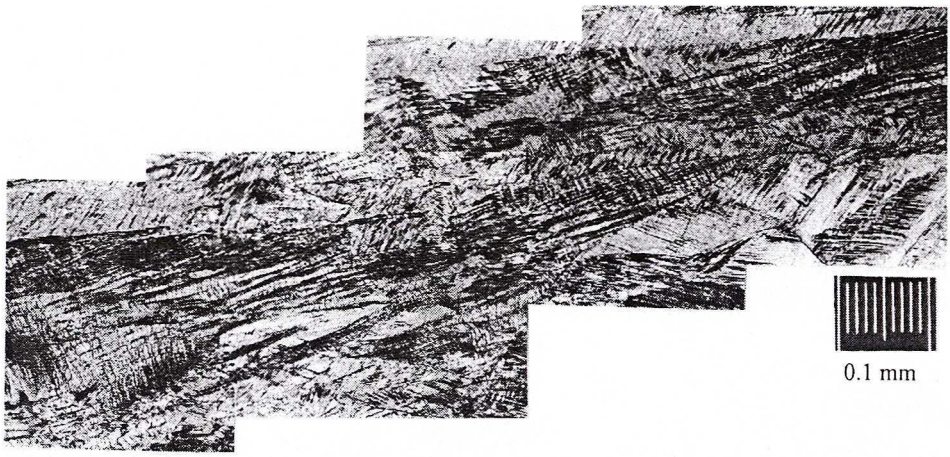

Fig. 18. Shear bends in CuSi3.5 silicon bronze at room temperature deformed to ε_p=0.8 with strain rate of 0,1 s^{-1} and strain amplitude of 0.2

changes of active slip systems and the dynamic recrystallization process occurs mainly in selected paths with high density of the slip bands and shear bands. Therefore during complex deformation the recrystallization is more heterogeneous than in simple deformation tests. The microstructure was composed with areas of high dispersion grains and grains with elongated shape somewhat smaller than the initial ones (Fig. 19). The elongated grains exist outside of slip and shear bands where the stored energy for DRX is no sufficient and dynamic restoration occurre mainly by dynamic recovery. Such behaviors of silicon bronze are in agreement with observation in the Nb-bearing steel, where the dynamic recrystallization is delayed by the strain reversal in torsion test [30].

Fig. 19. CuSi3.5 silicon bronze structure at temperature of 600 °C after complex deformation to ε_p=1.7 with strain rate of 0,1 s^{-1} and strain amplitude of 0.05

The effect of applied complex deformation on the limit plastic strain is quite different from the results obtained in the other works for cyclic deformation [6–9, 31]. The reason of such differences is that in the present work the angle between the strain tensors is equal 90° and dislocation structure is much different than in cyclic deformation where only reversal strain occur. From Figs. 14 and 15 it can be seen that the largest limit plastic strain was obtained for monotonic torsion and smallest one for monotonic tension, but for complex strain paths the limit plastic strain has a middle values.

Very interesting is the analysis of the relationship between the tensile flow stress-tensile plastic elongation selected out of complex deformation (Figs. 20 and 21). From these figures it can be clearly seen that additional stresses obtained in the cyclic torsion decrease the tensile flow stress. In the ambient temperature the decrease of tensile flow stress is proportional to the strain amplitude (Figure 20), but in the high temperature the decrease is nearly the same for all applied strain amplitudes (Figure 21).

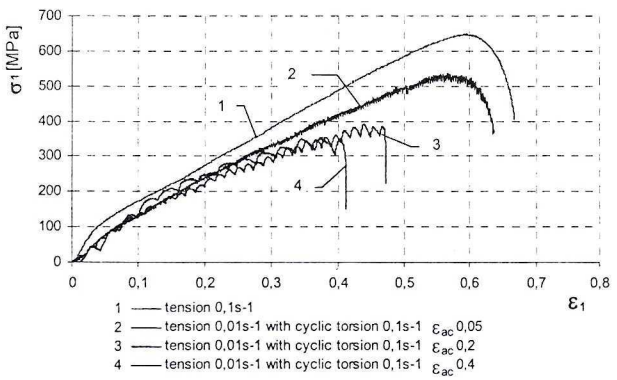

Fig. 20. The relationship between tensile stress σ_1 and elongation ε_1 in different complex deformation of CuSi silicon bronze at room temperature

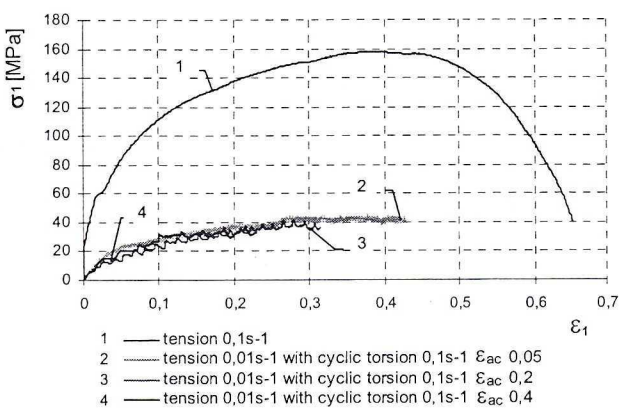

Fig. 21. The relationship between tensile stress σ_1 and elongation ε_1 in different complex deformation of CuSi silicon bronze at temperature of 600 °C

The obtained results are in qualitative agreement with Hubert-Mises yield criterion. The Huber-Mises yield surface shows that the additional principal stress, causes the decrease of the principal primary stress. From the Figures 20 and 21 it is clearly visible that cyclic torsion decrease the tensile plastic strain in complex deformation.

4. Conclusions

It has been found that complex strain paths have significant effect on the behaviour of CuSi3.5 silicon bronze during deformation. The minor cyclic torsion together with uniaxial tension in room temperature substantially decreases the equivalent flow stress in comparison with equivalent flow stress in monotonic tensile test in the range of deformation below plastic strain of 0.6 and in the case of torsion test below 1.2. The further increase of equivalent strain above these values caused slowly increases of the maximum values of equivalent flow stress in complex strain paths.

In the case of hot deformation at 600 °C the equivalent flow stresses for all applied strain paths are nearly the same beside the monotonic tensile where flow stress is highest. Decrease of amplitude of additional cyclic straining in complex deformation decreases the DRX process.

The additional reversal deformation intensifies localization in shear bands.

For FCC alloys with low SFE, like investigated silicon bronze, the twinning and crystallographic slip bands play very important role in mechanism of deformation.

Acknowledgements

The authors are grateful for the financial support from Polish Committee of Scientific Researches.

REFERENCES

[1] P.S. Bate, The effect of combined strain-path and strain-rate changes in aluminium, Metall. Trans. **A 24**, 2679–2689 (1993).

[2] S.B. Davenport, R.L. Higginson, Review, Strain path effect under hot working: an introduction, J. Mater. Process. Technol., 98, 267–291 (2000).

[3] M.G. Stout, A.D. Rollett, Large-strain Bauschinger effect in FCC metals and alloys, Metall. Trans. **A 21,** 3201–3213 (1990).

[4] A. Kocańda, Niskosykliczne zmęczenie stali SW7M o wysokiej twardości, Arch. Hut. **24,** 489 (1979).

[5] S. Kocańda, A. Kocańda, Niskocyklowa wytrzymałość zmęczeniowa metali, PWN, Warszawa 1989.

[6] J.P. Pinheiro, R. Barbosa, P.R. Cetlin, Dynamic restoration during the hot cyclic straining of copper, Scripta Mater. 38 53–57 (1998).

[7] J.P. Pinheiro, R. Barbosa, P.R. Cetlin, Effect of the cyclic straining amplitude on the hot dynamic restoration of copper, Scripta Mater. **44**, 187–193 (2001).

[8] J.P. Pinheiro, R. Barbosa, P.R. Cetlin, Warm cyclic straining of feritic interstitial free steel, Proc. of Symposium of Thermomechanical Processing of Steel, Ottawa, the Metallurgical Society of the Canadian Institute of Metallurgy, 221–233 Ottawa (2000).

[9] J.P. Pinheiro, R. Barbosa, P.R. Cetlin, The effect of cyclic torsion on the hot dynamic restoration of interstitial free steel in the austenitic range, J. Mater. Proc. Technol. **125-126**, 125–129 (2002).
[10] Z. Gronostajski, N. Misiołek, K. Jaśkiewicz, Wpływ małocyklowego skręcania oscylacyjnego na naprężenie uplastyczniające oraz odkształcenie graniczne brązu CuAl8, Materiały Konf. Forming'2002, 93–98 Luhacovicw (2000).
[11] Z. Gronostajski, N. Misiołek, The effect of amplitude in minor cyclic torsion on the behaviour of CuAl8 aluminium bronze, Proc. of Int. Sc. Conf. Achievements in Materials and Mechanical Engineering, AMME'2002, 219–222 Zakopane (2002).
[12] Z. Gronostajski, K. Jaśkiewicz, The effect of complex strain path on the hot dynamic restoration of CuSi3.5 silicon bronze, Proc. of Int. Sc. Conf. Achievements in Materials and Mechanical Engineering, AMME'2002, 215–218 Zakopane (2002).
[13] J. Pawlicki, F. Grosman, Naprężenie uplastyczniające w warunkach wymuszonej zmiany orientacji osi głównych stanu naprężenia wybranych materiałów metalicznych, Materiały Międzynarodowej Konf. FORMING'99, 208–213 (1999).
[14] J. Pawlicki, F. Grosman, Wpływ zmiany orientacji osi głównych stanu naprężenia na wartość naprężenia uplastyczniającego, Rudy i Metale Nieżelazne **42**, 501–503 (1997).
[15] J. Pawlicki, F. Grosman, Wpływ przebiegu odkształcania na wartość naprężenia uplastyczniającego polikryształów, Rudy i Met. Nieżelazne **10**, 565–568 (1999).
[16] E.S.C. Corr, M.T.P. Aguilar, P.R. Cetlin, The effect of tension/torsion strain path chenges on the work hardening of Cu Zn brass, J. Mat. Process. Technol **124**, 384–388 (2002).
[17] R.P. Singh, Structure of thermal – mechanical processed multiphase alloys, PhD thesis, Department of Materials Engineering, Drexel University, 1987.
[18] E. El-Danaf, S.R. Kalidindi, R.D. Doherty, Influence of deformation path on the strain hardening behavior and microstructure evolution in low SFE FCC metals, Int. J. of Plasticity **17**, 1245–1265 (2001).
[19] J.R. Cowan, R.L. Higginson, W.B. Hutchinson, P.S. Bate, Recrystallization following non-proportional straining in aluminium, Mater. Sci. Technol. **11**, 1104–1109 (1995).
[20] Z. Gronostajski, Analiza metodą elementów skończonych plastometrycznej próby skręcania, Informatyka w Technologii Materiałów **2**, 46–54 (2002).
[21] P.J. Hurley, P.D. Hodgson, B.C. Muddle, Analysis and characterization of ultra-fine ferrite produced during a new steel strip rolling process, Scripta Materialia **40**, 433–438 (1999).
[22] P.E. Armstrong, J.E. Hockett, Large strain multidirectional deformation of 1100 aluminium at 300 K, J. Mech. Phys. Solids **30**, 37–58 (1982).
[23] Z. Garczyński, Kształtowanie odkuwek metodą prasowania obwiedniowego, Materiały Konferencji Obróbka Plastyczna Metali'98, 29-34 Poznań-Kierz (1998).
[24] A. Piela, F. Grosman, Designing the Swaging Process, Proceedings of the 8th International Conference on Metal Forming 2000, 617–624 Kraków (2000).
[25] A. Korbel, W. Bochniak, Method of plastic forming of materials, US Patent No 5, 737.959 (1998).
[26] J. Gronostajski. J. et al., Plastometr realizujący złożone drogi odkształcania, Obróbka Plastyczna Metali, 12 5–10 (2001).
[27] Z. Gronostajski, Analiza wyznaczania naprężenia uplastyczniającego w próbie skręcania, Rudy i Metale Nieżelazne **44**, 236–242 (1999).
[28] E. Hadasik, A. Płachta, Z. Gronostajski, I. Schindler, Analiza sposobów wyznaczania naprężenia uplastyczniającego w próbie skręcania na gorąco, Int. Conf. Forming 2001, 77–84 Stara-Lesna (2001).
[29] Z. Gronostajski, Modele konstytutywne opisujące zachowanie się wybranych stopów miedzi w zakresie dużych odkształceń plastycznych, Prace Naukowe Instytutu Technologii Maszyn i Automatyzacji 75, Ser. Monografie, (2000) 1–225.
[30] R. Bartolomo, V.D. Jorge-Badiola, J.I. Astiazar and I. Gutisez, Flow stress behavior, static recrystallization and precipitation kinetics in a Nb-microalloyd steel after a strain reversal, Mater. Science and Eng. A **344**, 340–347 (2003).
[31] H. Ziemba, Ductility of metals under bidirectional cyclic torsion, Proc. of Int. Conf. On Challenges to Civil and Mechanical Engineering in 2000 end Beyond, 607-610 Wrocław (1997).

REVIEWED BY: WŁODZIMIERZ BOCHNIAK
Received: 20 November 2003.